DOI : 10.1016/j.scs.2020.102221

Methodologies to assess mean annual air pollution concentration combining numerical results and wind roses

Nicolas Reiminger[1,2*], Xavier Jurado[1,2], José Vazquez[2], Cédric Wemmert[2], Nadège Blond[3], Jonathan Wertel[1], Matthieu Dufresne[1]

[1]*AIR&D, 67000, Strasbourg, France*
[2]*ICUBE Laboratory, CNRS/University of Strasbourg, 67000, Strasbourg, France*
[3]*LIVE Laboratory, CNRS/University of Strasbourg, 67000, Strasbourg, France*
[*]*Corresponding author: Tel. +33 (0)6 31 26 75 88, Mail. nreiminger@air-d.fr*

Please cite this paper as : Reiminger, N., Jurado, X., Vazquez, J., Wemmert, C., Dufresne, M., Blond, N., Wertel, J., 2020. Methodologies to assess mean annual air pollution concentration combining numerical results and wind roses. Sustainable Cities and Society, 59, 102221. DOI: 1016/j.scs.2020.102221

ABSTRACT

Numerical models are valuable tools to assess air pollutant concentrations in cities which can be used to define new strategies to achieve sustainable cities of the future in terms of air quality. Numerical results are however difficult to be directly compared to air quality standards since they are usually valid only for specific wind speed and direction while some standards are on annual values. The purpose of this paper is to present existing and new methodologies to turn numerical results into mean annual concentrations and discuss their limitations. To this end, methodologies to assess wind speed distribution based on wind rose data are presented first. Then, methodologies are compared to assess mean annual concentrations based on numerical results and on wind speed distributions. According to the results, a Weibull distribution can be used to accurately assess wind speed distribution in France, but the results can be improved using a sigmoid function presented in this paper. It is also shown that using the wind rose data directly to assess mean annual concentrations can lead to underestimations of annual concentrations. Finally, the limitations of discrete methodologies to assess mean annual concentrations are discussed and a new methodology using continuous functions is described.

DOI : 10.1016/j.scs.2020.102221

1. Introduction

Over the past decades, outdoor air pollution has become a major issue, especially in highly densified urban areas where pollutant sources are numerous and air pollutant emissions high. In order to protect people from excessive exposure to air pollution, which can cause several diseases (Anderson et al., 2012; Kim et al., 2015), the World Health Organization (WHO) have recommended standard values that must not be exceeded for different pollutants such as nitrogen dioxide (NO_2) and particulate matter (EU, 2008; WHO, 2017) to protect population health, and the European Union (EU) decided to respect the same or other standards depending on the air pollutants. Among the different types of values given as standards, studies have shown that annual standards are generally more constraining and harder to reach than the other standards (Chaloulakou et al., 2008; Jenkin, 2004; Yuan et al., 2019).

In the meantime, recent studies have shown that the indoor air quality is strongly correlated with the outdoor one: while for nitrogen dioxide a 5% increase in indoor air pollutant concentrations can be expected for only a 1% increase in outdoor concentrations (Shaw et al., 2020), for particulate matters such as $PM_{2.5}$ the outdoor concentration can contribute from 27% to 65% of the indoor concentration (Bai et al., 2020). Being able to assess outdoor pollutant concentrations is therefore a necessity to improve air quality in the outdoor built environment, but also in the indoor one (Ścibor et al., 2019).

Annual concentrations can be assessed using both on-site monitoring and numerical modeling. On site monitoring requires measurements over long periods to be able to assess mean annual concentrations of pollutants, although a recent study has shown that mean annual concentration of NO_2 can be assessed using only one month of data (Jurado et al., 2020), which significantly reduces the measurement time required. Monitoring nonetheless has other limitations: it does not allow assessing the future evolution of the built environment or pollutant emissions, thus, limiting its applicability to achieve the smart sustainable cities of the future as defined by Bibri and Krogstie (2017). Numerical modelling can overcome these limitations and can help define new strategies to improve air quality in cities combining wind data, various air pollution scenarios and urban morphologies (Yang et al., 2020). Among the several models currently available, Computational Fluid Dynamics (CFD) has shown great potential for modeling pollutant dispersion from traffic-induced emissions by including numerous physical phenomena such as the effects of trees (Buccolieri et al., 2018; Santiago et al., 2019; Vranckx et al., 2015) and heat exchanges (Qu et al., 2012; Toparlar et al., 2017; Wang et al., 2011) on

DOI : 10.1016/j.scs.2020.102221

the scale of a neighborhood. However, this type of numerical result cannot be directly compared with the annual standards. Methodologies designed to assess mean annual concentrations based on numerical results can be found in the literature (Rivas et al., 2019; Solazzo et al., 2011; Vranckx et al., 2015), but further work is required to improve them and assess their limits.

The aim of this study is to provide tools and methodologies to assess mean annual concentrations based on numerical results and wind rose data to improve air quality in built environment and cities. It is firstly to evaluate whether it is possible to assess continuous wind speed distributions based on wind rose data. To do so, a statistical law called Weibull distribution is compared with a new sigmoid-based function built for the purpose of this study. Secondly, it is to present and compare a discrete methodology usually used to assess mean annual concentrations based on numerical results with a continuous methodology built for the purpose of this study, and to discuss their respective advantages and limitations. The data used for the wind speed distribution assessments, the area modeled and the CFD model used for illustration purposes are presented in Section 2. Then, the description and the comparison of the different methodologies are presented in Section 3 and, finally, a discussion is provided in Section 4.

2. Material and methods

2.1. Meteorological data

2.1.1. Data location

This work uses wind velocity and wind direction data from four cities in France. These cities were chosen to cover most of France to obtain representative results and include the cities of Strasbourg (Grand-Est region), Nîmes (Occitanie region), Brest (Bretagne region) and Lille (Hauts-de-France region). In particular, the data were obtained from the stations named Strasbourg-Entzheim, Nîmes-Courbessac, Brest-Guipavas and Lille-Lesquin, respectively. The location of these stations and their corresponding regions are presented in Fig. 1.

DOI : 10.1016/j.scs.2020.102221

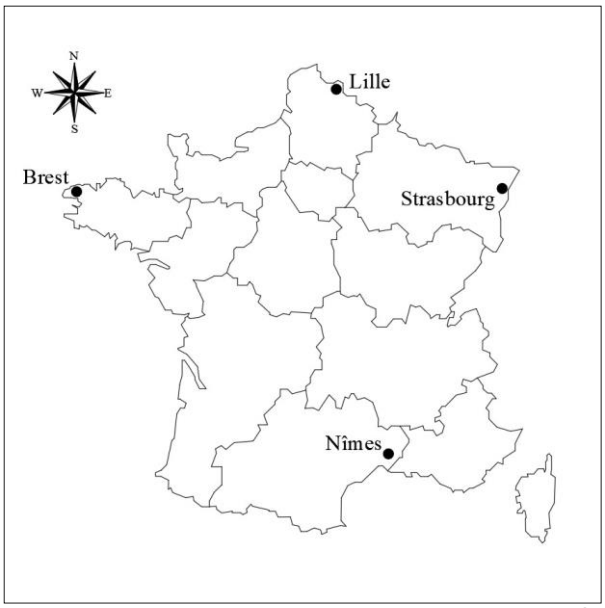

Fig. 1. Location of the different meteorological stations used.

2.1.2. Data availability and data range

The data used in this work were provided by Météo-France, a public institution and France's official meteorology and climatology service. The data are mainly couples of wind velocity and wind direction over a twenty-year period from 1999 to 2018, except for the Strasbourg-Entzheim station where it is a ten-year period from 1999 to 2008. The data were obtained via a personal request addressed to Météo-France and were not available on open-access. A summary of the information of the stations is presented in Table 1, with the time ranges of the data and the number of data available (the coordinates are given in the World Geodetic System 1984).

Table 1. Summary of the available data.

Station				Data availability		
Location	Latitude	Longitude	Altitude	Time range	Number of valid cases	Number of missing cases
Brest - Guipavas	48°27'00"N	4°22'59"O	94 m	2009 - 2018	29,171	45
Lille - Lesquin	50°34'12"N	3°05'51"E	47 m	2009 - 2018	29,185	31
Nîmes - Courbessac	43°51'24"N	4°24'22"E	59 m	2009 - 2018	29,214	2
Strasbourg - Entzheim	48°32'58"N	7°38'25"E	150 m	1999 - 2008	29,199	25

All the data were monitored from wind sensors placed 10 meters from the ground and the wind frequencies are available for each wind direction with 20° steps for two distinct wind discretizations: a "basic" discretization giving wind frequencies for 4 velocity ranges (from 0 to 1.5 m/s, 1.5 to 3.5 m/s, 3.5 to 8 m/s and more than 8 m/s), illustrated in Fig. 2. (A); and a "detailed" discretization giving wind frequencies by 1 m/s steps except between 0 and 0.5 m/s,

DOI : 10.1016/j.scs.2020.102221

illustrated in Fig. 2. (B). The “basic” discretization is a common format mostly found in wind roses (possibly with different velocity ranges) while the “detailed” data are less common and more expensive.

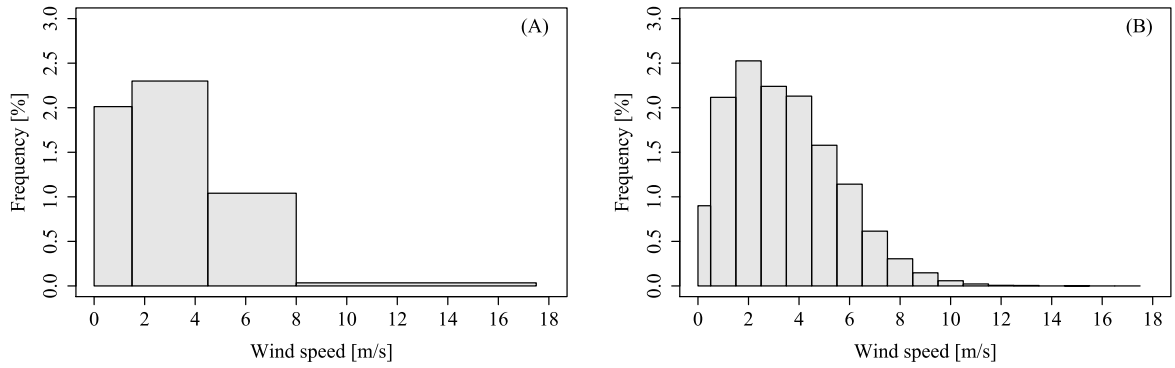

Fig. 2. Examples of data for Strasbourg and a 200° wind direction with (A) only 4 ranges of velocities and (B) the detailed data discretized in 18 ranges.

The wind roses for each meteorological station considered in this work and based on the “basic” 4-velocity-range discretization described in Fig. 2. (A) are provided in Fig. 3. This figure shows how the monitoring locations considered in this study give distinct but complementary information, with for example many high velocities at Brest compared to Strasbourg and Nîmes, where almost no velocities were monitored over 8 m/s, and with dominant wind directions at Nîmes and Strasbourg compared to the other stations.

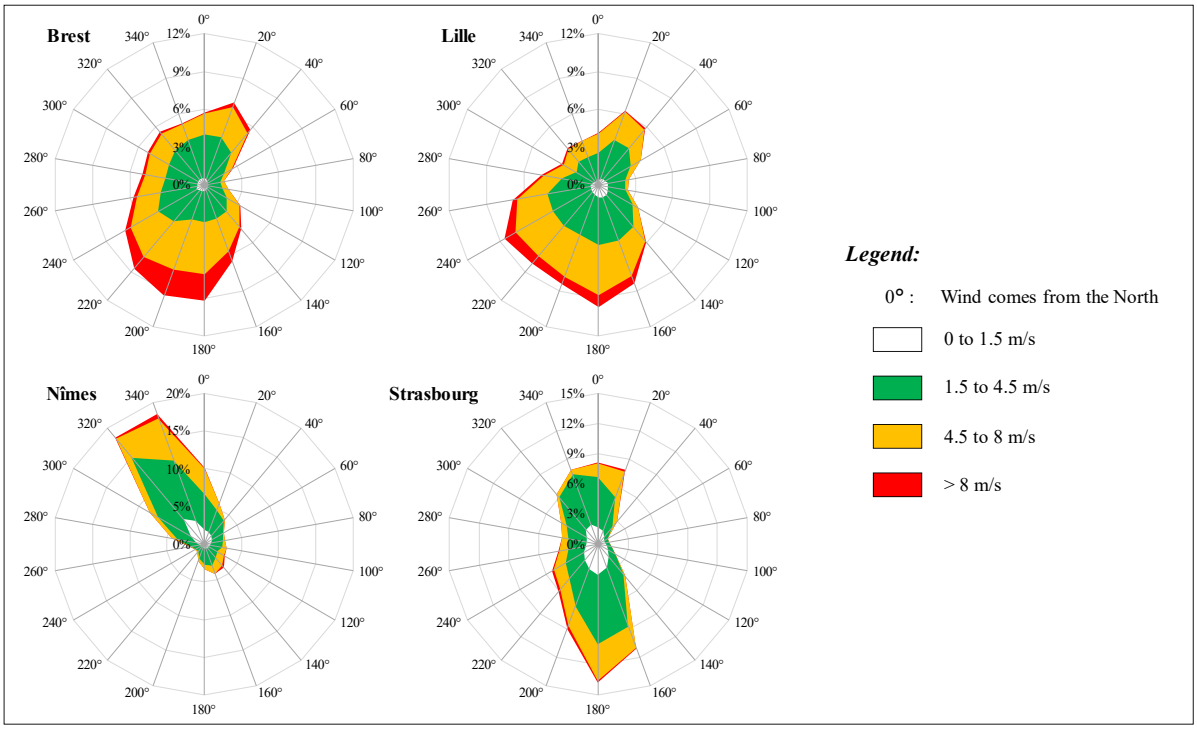

Fig. 3. Wind roses for each location considered.

DOI : 10.1016/j.scs.2020.102221

121

122 *2.1.3. Interpolation functions*

123 A two-parametric continuous probability function, the Weibull distribution, mainly used in the
124 wind power industry, can be used to describe wind speed distribution (Kumar et al., 2019;
125 Mahmood et al., 2019). The equation of the corresponding probability density function is given
126 in (1).

127 $$f(v) = \frac{k}{\lambda}\left(\frac{v}{\lambda}\right)^{k-1} e^{-(v/\lambda)^k} \qquad (1)$$

128 where v is the wind velocity, k is the shape parameter and λ is the scale parameter of the
129 distribution, with k and λ being positive.

130 For the purpose of this study, an original 5-parametric continuous function was built to
131 determine the "detailed" wind discretization based on the "basic" 4-velocity-range wind
132 discretization. This function, called Sigmoid function, based on the composition of two sigmoid
133 functions, is given in (2). The two functions will be compared in the results section.

134 $$f(v) = \alpha.\left(-1 + \frac{1}{1+\beta_1.e^{-\gamma_1.v}} + \frac{1}{1+\beta_2.e^{\gamma_2.v}}\right) \qquad (2)$$

135 where α, β_1, β_2, γ_1 and γ_2 are positive parameters.

136

137 2.2. Numerical model

138 Simulations were performed using the unsteady and incompressible solver *pimpleFoam* from
139 OpenFOAM 6.0. A Reynolds-Averaged Navier-Stokes (RANS) methodology was used to solve
140 the Navier-Stokes equations with the RNG k-ε turbulence model, and the transport of
141 particulate matter was performed using a transport equation. This solver was validated
142 previously in Reiminger et al. (2020).

143 The area chosen to illustrate the methodologies discussed in this paper is located in
144 Schiltigheim, France (48°36'24", 7°44'00"), a few kilometers north of Strasbourg. This area, as
145 well as the only road considered as an emission source in this study (D120, rue de la Paix), are
146 illustrated in Fig. 4. (A). PM_{10} traffic-related emissions were estimated at 1.39 mg/s using daily
147 annual mean traffic and were applied along the street considering its length in the numerical
148 domain (200 m), its width (9 m) and an emission height of 0.5 m to take into account initial
149 dispersion.

DOI : 10.1016/j.scs.2020.102221

The recommendations given by Franke et al. (2007) were followed. In particular, with H being the highest building height (16 m), the distances between the buildings and the lateral boundaries are at least $5H$, the distances between the inlet and the buildings as well as for the outlet and the buildings are at least $5H$ and the domain height is around $6H$. An illustration of the resulting 3D sketch is presented in Fig. 4. (B). A grid sensitivity test was performed and showed that hexahedral meshes of 1 m in the study area and 0.5 m near the building walls are sufficient, leading to a more comparable resolution than other CFD studies (Blocken, 2015) and leading to a total number of around 800,000 cells. The resulting mesh is illustrated in Fig. 5.

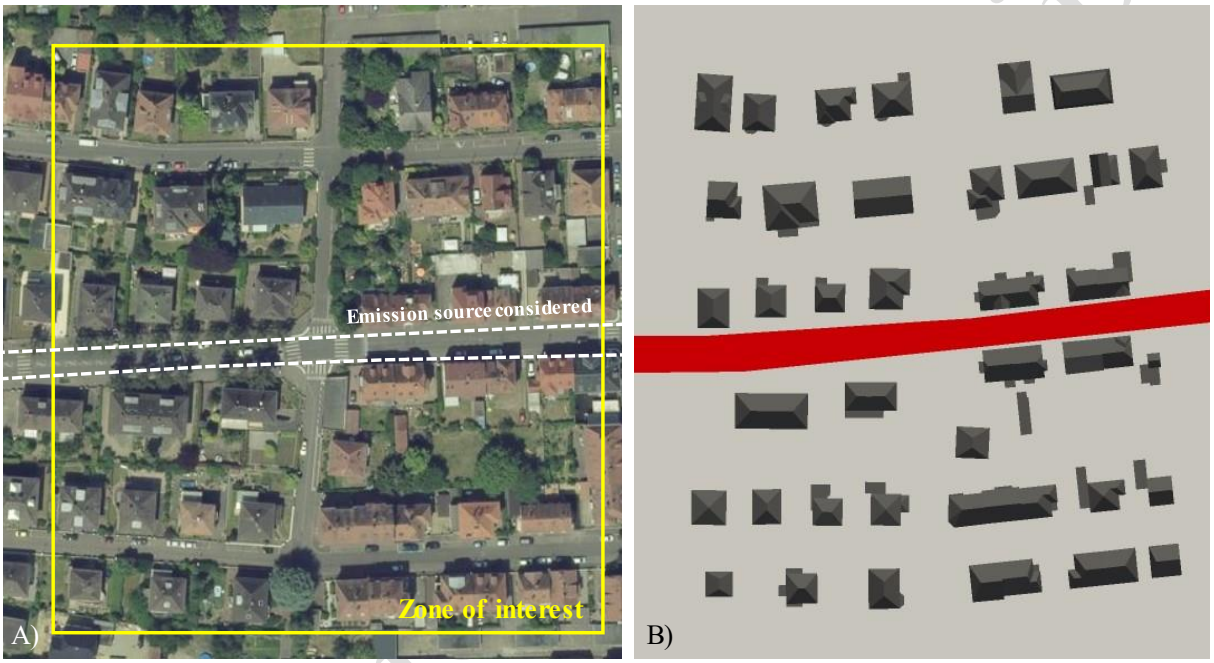

Fig. 4. Illustration of (A) the area of Strasbourg modeled with the road considered for the traffic-related emissions (white dashed lines), and (B) the corresponding area built in 3D for the numerical simulations with the emission source (red).

No-slip conditions (U = 0 m/s) were applied to the building walls and ground, and symmetry conditions to the lateral and the top boundaries. A freestream condition was applied to the outlet boundary, and neutral velocity, turbulent kinetic energy and turbulent dissipation profiles suggested by Richards and Norris (2011) were applied to the inlet boundary.

A total of 18 simulations were performed using the same wind velocity ($U_{10\,m}$ = 1.5 m/s) but with different wind directions from 0° to 340° using a 20° step. Since the simulations were performed in neutral conditions and without traffic-induced turbulence, the dimensionless concentration C^* given in (3) is a function only of the wind direction (Schatzmann and Leitl, 2011). In other words, this means that considering the previous hypothesis, and for a given

DOI : 10.1016/j.scs.2020.102221

emission and building configuration (leading to constant $H.L/q$ ratio), only one simulation is needed for each wind direction simulated. The pollutant concentrations for a non-simulated wind velocity u can therefore be computed using (4).

$$C^* = \frac{C.U.H.L}{q} \qquad (3)$$

where C^* is the dimensionless concentration, C is the concentration, U the wind velocity, H the characteristic building height and q/L the source strength of emission.

$$C_u = U_{ref}.\frac{C_{ref}}{u} \qquad (4)$$

where C_u is the pollutant concentration for the wind velocity u not simulated and C_{ref} the pollutant concentration for the simulated wind velocity U_{ref}.

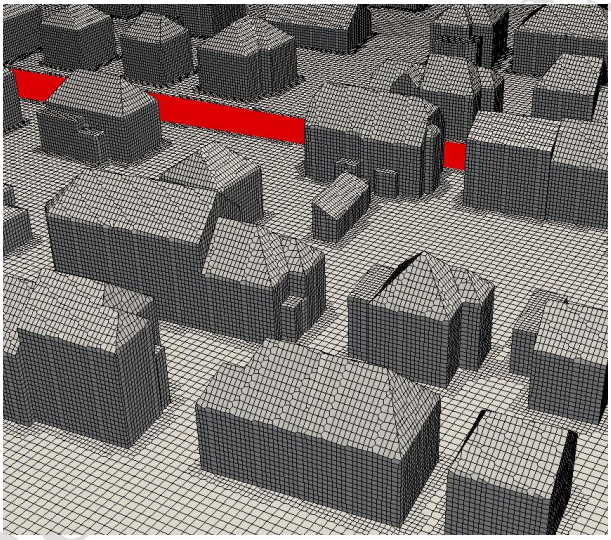

Fig. 5. Illustration of the meshes in the computational domain with the emission source (red), with 0.5 m meshes near the buildings and 1 m in the study area.

3. Results

3.1. Wind data interpolation

3.1.1. Comparison between the Weibull distribution and the sigmoid function

The best fitting parameters of the two functions were determined for the whole dataset using a non-linear solver and the "basic" 4-velocity-range wind data. The solver was set up to solve equation (5) for the four-velocity ranges [0, 1.5[, [1.5, 4.5[, [4.5, 8[and [8, +∞[for both Weibull and sigmoid functions. This equation reflects that the sum of the frequencies between two wind velocities (i.e. the area under the curve) must be equal to the frequency given in the "basic" 4-

DOI : 10.1016/j.scs.2020.102221

velocity-range wind data. Since the sigmoid function has five parameters, a fifth equation to be solved was added only for this function and corresponds to (6). With this equation, it is assumed that the wind frequency tends toward 0% when the wind speed tends toward 0 m/s, as for the Weibull distribution.

$$\int_a^b f(v).dv = FVR_{[a;b[} \qquad (5)$$

$$f(0) = 0 \qquad (6)$$

where $f(v)$ is the Weibull or the sigmoid function and $FVR_{[a;b[}$ is the wind frequency given in the 4-velocity-range data for wind velocities ranging from a included to b excluded.

Fig. 6 (A–D) shows a comparison between the Weibull distribution, the sigmoid function and the "detailed" 18-velocity-range data for one wind direction of each meteorological station. According to these figures, the two functions generally give the same trends, and both appear to give a good estimation of the "detailed" wind data. However, depending on the case, the Weibull function can provide improvements in comparison to the sigmoid function, as in Fig. 6. (A), or vice versa, the sigmoid function can provide improvements in comparison to the Weibull function, as in Fig. 6. (D).

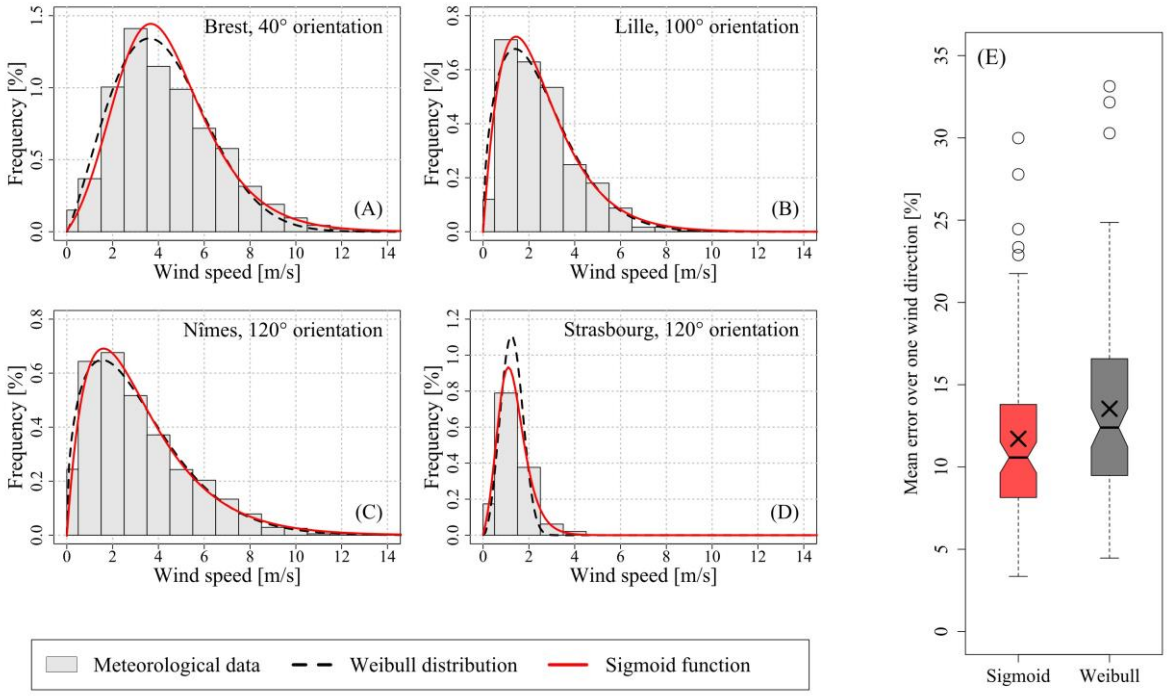

Fig. 6. (A–D) Weibull distribution and sigmoid function results compared to the detailed meteorological wind frequency data for one wind direction at each station considered and (E) a notched box plot of the mean error over one wind direction with all stations included for both functions.

DOI : 10.1016/j.scs.2020.102221

To better compare the two functions, a notched box plot of the mean error over one wind direction is given in Fig. 6. (E). According to this figure, the sigmoid function gives generally better results compared to the Weibull distribution, with a lower maximal error (30.0% and 33.1% respectively); a lower first quartile (8.1% and 9.5% resp.); a lower third quartile (13.8% and 14.5% resp.); a lower mean (11.7% and 13.5% resp.); and a lower median (10.6% and 12.4% resp.). The differences are, however, small and may not be significant, especially for the median because the notches slightly overlap. These differences between the Weibull distribution and the sigmoid function are also location dependent, with for example better prediction of the wind distribution in Strasbourg using the sigmoid function and an equivalent prediction in Brest. Finally, it should be noted that both functions can lead to underestimations of the lower wind velocity frequencies, as shown in Fig. 6. (A) and (D).

According to the previous results, the Weibull distribution and the sigmoid function can accurately reproduce the "detailed" wind distribution based on a "basic" 4-velocity-range discretization with an average error of around 12% over the four stations considered in France. They can nonetheless lead to underestimations of the low wind velocity frequencies, for which the highest pollutant concentrations appear.

3.1.2. Optimization of the sigmoid function interpolation for low wind velocities

The parametrization of the sigmoid function, called standard sigmoid function, was modified to improve the estimation of the low wind velocity frequencies in order to avoid underestimating pollutant concentrations.

Based on all the meteorological data considered in this study, it was found that the underestimation of low wind velocity frequencies occurs mostly when the frequency of the first velocity range is lower than the frequency of the second velocity range. In this specific case, the optimized sigmoid function still needs the equation (5) for the four-velocity ranges given in the "basic" wind data, but equation (6) is replaced by equation (7); otherwise, the previous parametrization using equations (5) and (6) is kept.

$$f(0) = FVR_{[0;\alpha[}\frac{FVR_{[0,\alpha[}}{FVR_{[\alpha,\beta[}} \qquad (7)$$

DOI : 10.1016/j.scs.2020.102221

where $FVR_{[0,\alpha[}$ is the wind frequency for the first range of velocities given in the 4-velocity-range data and $FVR_{[\alpha,\beta[}$ is the wind frequency for the second range of velocities (e.g., in this study α = 1.5 and β = 4.5).

The methodology for the optimized sigmoid function is illustrated in Fig. 7. (A–B): when the frequency of the first velocity range is higher than the second, as in Fig. 7. (A1), the standard parametrization of the sigmoid function can be used because the low wind velocity frequencies are estimated accurately, as in Fig. 7. (A2), when the frequency of the first velocity range is lower than the second, as in Fig. 7. (B1), the standard parametrization leads to underestimations of low wind velocity frequencies and the optimized parametrization should be used instead, leading to a better estimation of the frequencies, as shown by the blue curve in Fig. 7. (B2) compared to the red curve.

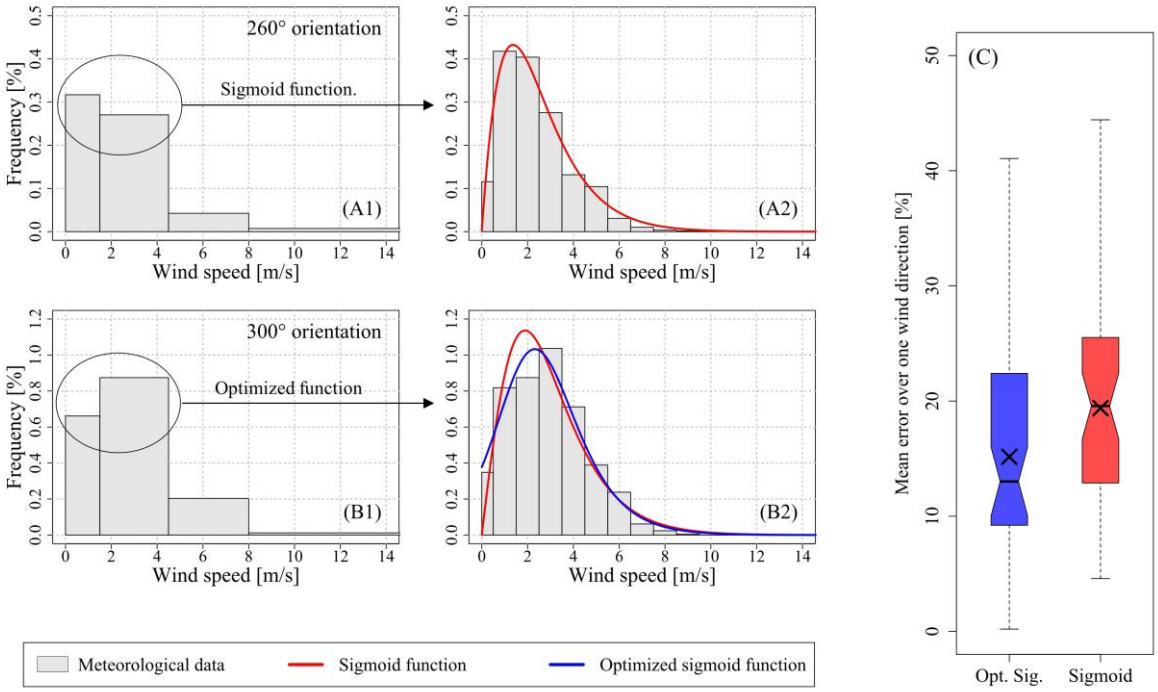

Fig. 7. (A–B) Illustration of the optimized sigmoid function methodology and (C) comparison with the standard sigmoid function results.

The improvements with the optimized sigmoid function compared to the standard function was assessed and the results are presented in Fig. 7. (C). For this comparison, only the wind directions where the optimized function was applied are considered (49 wind directions within the 78 previously used) and the errors compared to the "detailed" 18-velocity-range data were calculated for the low wind velocity frequencies (between 0 and 3.5 m/s). According to this figure, the optimized sigmoid function gives improvements over the standard sigmoid function

DOI : 10.1016/j.scs.2020.102221

with a lower maximal error (41.0% and 44.4% respectively); a lower first quartile (9.2% and 12.9% resp.); a lower third quartile (22.4% and 25.5% resp.); a lower mean error (15.2% and 19.4% resp.); and a lower median (13.0% and 19.6% resp.). The improvements using the optimized function are significative, in particular for the median since the box plot notches do not overlap; they are also location dependent. A global improvement of the wind distribution prediction ranging between 20% and 45% is observed in Strasbourg, Lille and Nîmes while no improvement is observed in Brest.

According to the previous results, using the optimized sigmoid function can improve the reproduction of the "detailed" wind distribution based on a "basic" 4-velocity-range compared to the standard sigmoid function, especially for low wind velocities.

3.2. Mean annual concentration assessment

3.2.1. Discrete methodology with intermediate velocities

Initially, mean annual concentrations based on the CFD results can be calculated using a discrete methodology. This methodology considers that the mean annual concentration at a given location is composed of several small contributions of different wind velocities and wind directions. The mean concentration over one wind direction can be calculated with equation (8) and the mean annual concentration with equation (9). A similar methodology can be found in Solazzo et al. (2011) or in Rivas et al. (2019).

$$\bar{C}_d = \frac{\sum_{r=1}^{n} C_{d,r} \cdot f_{d,r}}{\sum_{r=1}^{n} f_{d,r}} + C_{bg} \quad (8)$$

$$\bar{C} = \frac{\sum_{i=1}^{n} \bar{C}_d \cdot f_d}{\sum_{i=1}^{n} f_d} \quad (9)$$

where $\bar{C}_d$ is the mean concentration over one wind direction, $C_{d,r}$ is the concentration for a given wind direction d and a given wind velocity range r, $f_{d,r}$ is the frequency for a given wind direction and a given wind velocity range, C_{bg} is the background concentration, $\bar{C}$ is the mean annual concentration and f_d the total frequency of a given wind direction.

With this methodology, it is necessary to choose a wind velocity in each velocity range for which the concentration will be calculated based on the CFD result. A simple choice is to consider an intermediate velocity, noted v_i, corresponding to the average between the minimal

DOI : 10.1016/j.scs.2020.102221

and the maximal value of the velocity range (e.g., for the velocity range [1.5, 4.5[, the intermediate value is 3 m/s).

A comparison of results for this methodology is given in Fig. 8. with distinct cases considering (A) the "basic" 4-velocity-range frequencies, (B) the "detailed" 18-velocity-range frequencies, (C) the frequencies calculated with the sigmoid function, and (D) the frequencies calculated with the optimized sigmoid function. No background concentration is considered in this study to permit better comparison of the results and the CFD results used as inputs for the methodologies were strictly the same.

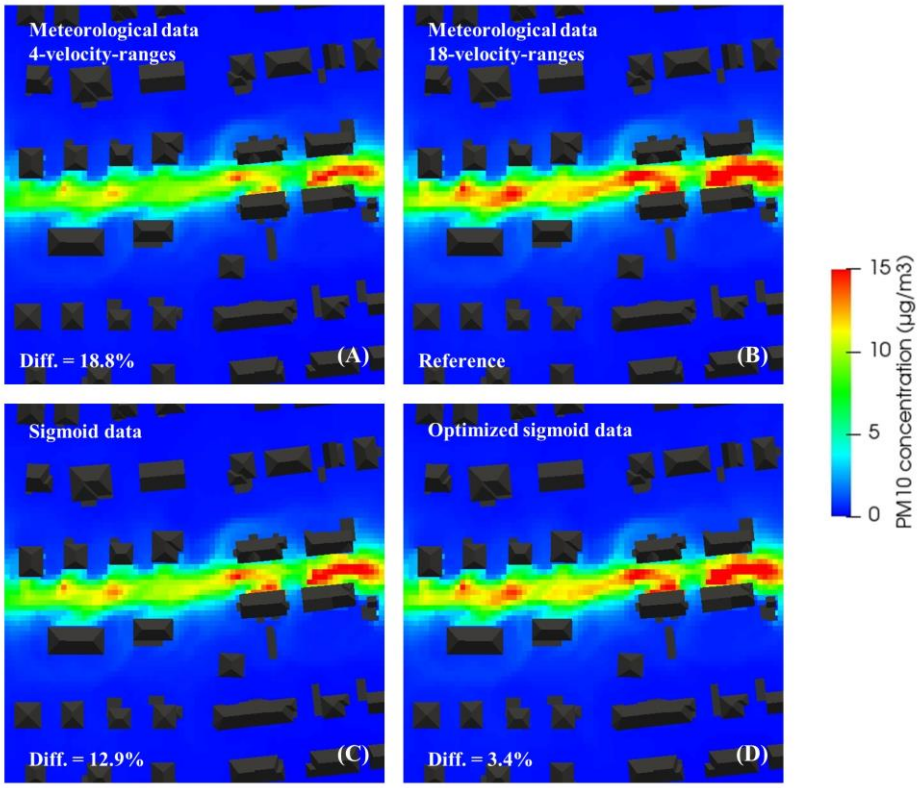

Fig. 8. Mean annual concentrations without background concentration based on (A) the "basic" 4-velocity-range monitoring data, (B) the "detailed" 18-velocity-range monitoring data, (C) the sigmoid interpolation data and (D) the optimized sigmoid interpolation data.

Initially, it can be seen that using the "basic" 4-velocity-range data leads to an underestimation of the concentrations compared to the case using "detailed" 18-velocity-range data by around 19%. When calculating the "detailed" wind velocity distribution based on the "basic" data with the sigmoid function, the difference is reduced to 12.9%. Finally, the best results are obtained when using the optimized sigmoid function with an underestimation of 3.4%. According to these results, using the "basic" 4-velocity-range frequencies can give an estimation of the mean annual concentrations but is not sufficient to reach good accuracy compared to the mean annual

DOI : 10.1016/j.scs.2020.102221

concentration calculated with the "detailed" wind velocity distribution. However, using the sigmoid function and especially the optimized variant significatively improves the results, leading to almost the same results as those obtained with the "detailed" wind velocity distribution.

3.2.2. Discrete methodology with representative velocities

The previous methodology used to compute annual concentrations, which was easy to set up, nonetheless has certain weaknesses that mostly concern the choice of the wind velocity for which the concentrations will be calculated, based on the CFD results. Using an intermediate velocity v_i corresponding to the average between the minimal and the maximal value of the velocity range can lead to underestimations of the mean annual concentrations. Indeed, in doing so, it is implicitly assumed that the concentration is constant with the wind velocity in a given wind velocity range. However, the concentration is not constant within a velocity range, especially when this range is large. A function describing the evolution of the concentration depending on the wind speed is therefore needed. As an example, for neutral atmosphere usually assumed in CFD, the concentration evolves hyperbolically with velocity according to equation (4). The representative velocity over one velocity range, considering the hyperbolic evolution of the concentration, is given in (11) as a result of (10) and (4).

$$\frac{1}{2}\int_{v_{min}}^{v_{max}} c(v).dv = \int_{v_{min}}^{v_r} c(v).dv \quad (10)$$

$$v_r = \sqrt{\frac{2}{\frac{1}{{v_{max}}^2} + \frac{1}{{v_{min}}^2}}} \quad (11)$$

where v_{max} and v_{min} are respectively the maximal and the minimal velocities of the velocity range, v_r is the representative velocity of the velocity range and $c(v)$ the equation describing the evolution of the concentration as a function of the wind velocity, i.e. equation (4).

The representative velocities v_r were calculated with equation (11) and compared to the intermediate velocities v_i. It is noteworthy that for a velocity range with a minimal velocity of 0 m/s, it is mathematically not possible to compute the representative velocity due to the domain definition of the function. A choice is therefore required; for the purpose of this study, the same ratio v_r/v_i as for [0.5, 1.5[was considered.

DOI : 10.1016/j.scs.2020.102221

According to the results summarized in Table 2. for wind velocities ranging from 0 to 6.5 m/s, the intermediate velocity can be much higher than the representative velocity for low velocities. For example, for wind velocities ranging from 0.5 to 1.5 m/s, the intermediate velocity of 1 m/s is almost twice as high as the representative velocity of 0.67 m/s. For higher velocity ranges, such as [2.5, 3.5[or more, the differences can be neglected. This last statement is true for 1 m/s steps between the minimal and the maximal velocities of the velocity range but can become wrong for higher velocity steps.

Table 2. Comparison between the intermediate velocity v_i and the representative velocity v_r (*: the representative velocity was calculated considering the same ratio v_r/v_i as for [0.5, 1.5[ ).

v_{min} [m/s]	0	0.5	1.5	2.5	3.5	4.5	5.5
v_{max} [m/s]	0.5	1.5	2.5	3.5	4.5	5.5	6.5
v_i [m/s]	0.25	1.00	2.00	3.00	4.00	5.00	6.00
v_r [m/s]	0.1675*	0.67	1.82	2.88	3.90	4.92	5.94
v_r/v_i	0.67*	0.67	0.91	0.96	0.97	0.98	0.99

Fig. 9. shows a comparison of the mean annual concentrations when using the intermediate velocity and when using the representative velocity, based on the “detailed” 18-velocity-range wind distribution. According to the results, using the intermediate velocity leads to considerable underestimations of the mean annual concentrations compared to the use of the representative velocity. The underestimation is about 20%. When using the discrete methodology presented in Section 3.2.1., it is therefore suggested to use the representative velocity instead of the intermediate velocity to better take into account the hyperbolic evolution of the pollutant concentrations with the wind velocity to avoid underestimating the concentrations.

DOI : 10.1016/j.scs.2020.102221

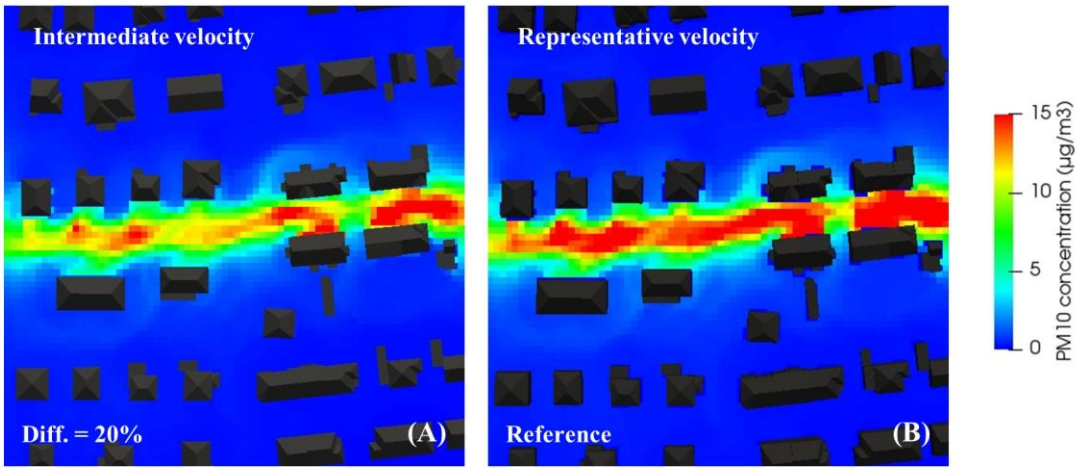

Fig. 9. Comparison of the mean annual concentrations based on the "detailed" 18-velocity-range wind distribution using (A) the intermediate velocity and (B) the representative velocity.

Lastly, it should be noted that the representative velocities given previously were calculated with the assumption of equation (4) applied to equation (10). If the function describing the evolution of the concentration with the wind speed would change, e.g. for other types of numerical models or atmospheric conditions, equation (10) would need to be solved again with the new function to have a representative velocity adapted to the conditions and the numerical model considered.

3.2.3. Continuous methodology using the sigmoid function

For the last approach, mean annual concentrations based on CFD results can be calculated using a continuous methodology. This methodology is a combination of equation (4), describing the evolution of pollutant concentration with wind velocity, and equation (2), describing the evolution of wind velocity frequency with wind velocity. The equation to compute the mean annual concentrations continuously is given in (12). The annual concentration can then be calculated using (9).

$$\bar{C}_d = \frac{\int_0^{+\infty} c(v).f(v).dv}{\int_0^{+\infty} f(v).dv} + C_{bg} \quad (12)$$

where $\bar{C}_d$ is the mean annual concentration for a given wind direction, $c(v)$ is the function describing the evolution of the concentration with the wind velocity, $f(v)$ is the function describing the evolution of the wind velocity frequency with the wind velocity, and C_{bg} is the background concentration.

DOI : 10.1016/j.scs.2020.102221

Taking equation (4) for $c(v)$ and equation (2) for $f(v)$ leads to a mathematical problem. Indeed, $c(v)$ is not defined for v = 0 and the limit of $c(v).f(v)$ tends toward infinity when v tends toward 0. To avoid this problem, equation (13) is suggested instead of equation (12). With this equation, it is considered that a minimal velocity (v_{min}) exists for which the pollutant concentration will no longer increase when the wind velocity decreases. This hypothesis can be justified by the additional effects, such as traffic-induced turbulence (Vachon et al., 2002) and atmospheric stability (Qu et al., 2012) that may participate in pollutant dispersion for low wind velocities or become preponderant. We suggest applying a constant pollutant concentration for wind velocities ranging from 0 to v_{min} and suggest using $C_{max} = c(v_{min})$. The choice of v_{min} is particularly important when using the optimized sigmoid function.

$$\bar{C_d} = C_{max}.\frac{\int_0^{v_{min}} f(v).dv}{\int_0^{+\infty} f(v).dv} + \frac{\int_{v_{min}}^{+\infty} c(v).f(v).dv}{\int_0^{+\infty} f(v).dv} + C_{bg} \quad (13)$$

where $\bar{C_d}$ is the mean annual concentration for a given wind direction, C_{max} is the maximal concentration accepted for the calculation, v_{min} is the velocity under which $c(v)$ is considered equal to C_{max}, $f(v)$ is equation (2), $c(v)$ is equation (4) and C_{bg} is the background concentration.

Fig. 10. shows a comparison between the discrete methodology with the representative velocities and the continuous methodology using the optimized sigmoid function. It can be seen that the results of the discrete methodology given in Fig. 10. (A) can be reached by the continuous methodology. Nonetheless, the difference of 5% reached using v_{min} = 0.01 m/s can increase when changing the value of v_{min}: lower values will lead to higher concentrations whereas higher values will lead to lower concentrations. The value of v_{min} must therefore be chosen carefully.

DOI : 10.1016/j.scs.2020.102221

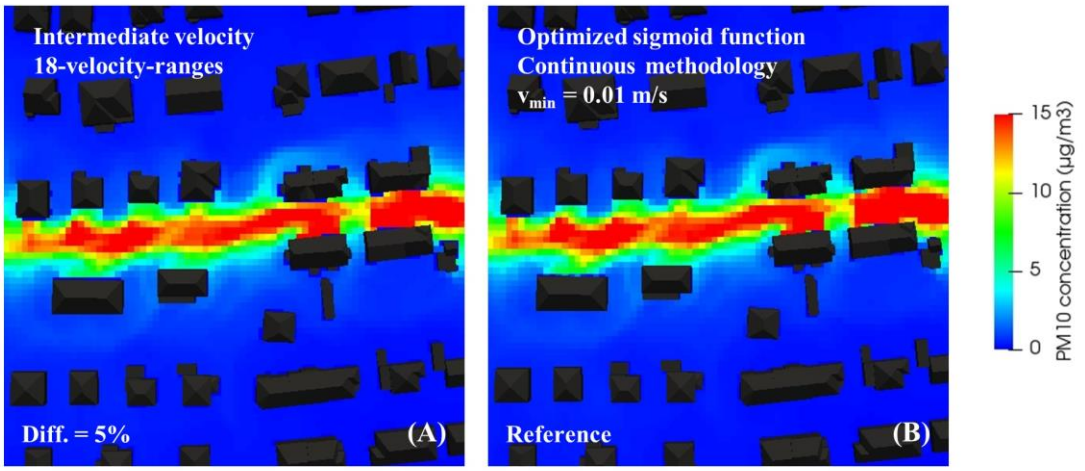

Fig. 10. Comparison of the mean annual concentrations (A) based on the "detailed" 18-velocity-range wind distribution and using the intermediate velocity, and (B) based on the optimized sigmoid function and v_{min} = 0.01 m/s.

4. Discussion

This study provides tools to assess wind velocity distributions based on "basic" data and mean annual air pollutant concentrations based on CFD results. Additional work should be done to improve the methodologies and the major issues are discussed hereafter.

The capability of the Weibull and the sigmoid functions to describe wind velocity distribution was assessed based on wind data from four meteorological stations in France. All of these stations were located in peri-urban environments close to large French cities. It is necessary to take into account that the results, and especially the interpolation-related errors, might be different for other types of stations such as urban and rural stations, and for other countries with different wind characteristics. In particular, the optimization suggested for the sigmoid function may not be suitable for different countries or type of station. Further works are therefore required in this direction.

The mean annual atmospheric pollutant concentrations can be calculated using a discrete methodology as done Solazzo et al. (2011) or Rivas et al. (2019). However, this methodology has two major problems. The first concerns the choice of wind velocity for which the pollutant concentrations will be calculated: choosing an intermediate velocity is a simple approach which can lead to considerable underestimations of pollutant concentrations, and it is better to use a representative velocity instead, as suggested in this paper. Using the representative velocity requires, however, making a choice for the first velocity range. The second problem concerns the velocity step used to build the wind velocity ranges: the result depends on the velocity step

DOI : 10.1016/j.scs.2020.102221

used, especially for the lower wind velocities for which a decrease in the velocity-step leads to higher mean annual concentrations. To avoid these two problems, a continuous methodology has been proposed. This methodology does not have an intrinsic limitation, but dependent on the function describing the evolution of the concentration as a function of wind velocity. If we consider a hyperbolic evolution of the concentration with wind velocity, it is necessary to choose a minimal value of velocity for which it is considered that lower velocities will not increase the concentrations due to compensatory phenomena (traffic-induced turbulence, atmospheric stability, etc.). The value of the minimal velocity is open to discussion and assessing this value is outside the scope of this paper. Further works are required, for example with infield measurement campaigns and comparisons between mean annual concentrations monitored and calculated with the continuous methodology. Lastly, two methodologies therefore exist, a discrete and a continuous with the discrete one being easier to implement in a code. However, we suggest using the continuous methodology if the user can describe the evolution of the concentration with the wind speed using a given piecewise continuous function. The discrete methodology can also be employed but, when an intermediate velocity is used, the user should be aware that the assumption of a constant pollutant concentration within velocity the range is made. To avoid this assumption, the user could consider a representative velocity instead, with as an example a linear evolution of the concentration between the limits of the velocity ranges.

Finally, it should be noted that the methodologies to assess mean annual concentrations were addressed using CFD results implying a neutral atmosphere, but can be used for any numerical results as long as a function describing the evolution of the concentration with the wind velocity is available.

5. Conclusion

The objectives of this study were to provide methodologies; (1) to assess wind velocity distribution based on “basic” data, and (2) to assess mean annual air pollutant concentrations based on numerical results. Three approaches for each objective were described and compared throughout this paper and the main conclusions are as follows:

(1.a) The Weibull distribution and the sigmoid function can both accurately reproduce “detailed” 18-velocity-range wind distribution based on “basic” 4-velocity-range wind data with an average error of 12%. These functions can nonetheless underestimate the frequencies of low velocities.

DOI : 10.1016/j.scs.2020.102221

(1.b) The optimized sigmoid function improves the wind distribution results over the standard sigmoid function, especially for low wind velocities.

(2.a) Using "basic" 4-velocity-range wind data and the discrete methodology can provide an estimation of the mean annual concentrations but is not sufficient to achieve high precision, leading to a difference of around 19% compared to the use of "detailed" 18-velocity-range wind data. Using the sigmoid function instead, based on the "basic" wind data improves the mean annual concentration results with a global error of less than 4%.

(2.b) When using the discrete methodology to assess mean annual concentrations, it is suggested to use a representative velocity of the function describing the evolution of pollutant concentrations with the wind velocities instead of an intermediate velocity. The intermediate velocity leads to underestimations of mean annual concentrations, especially when using CFD results with a neutral case hypothesis where the concentration evolves hyperbolically with the wind velocity.

(2.c) Mean annual concentrations can be assessed using a continuous methodology that does not have any of the limitations of discrete methodologies. It is, however, limited by the function describing the evolution of the concentrations with the wind velocities, which leads to the need to choose a minimal velocity when using the sigmoid function.

Finally, the methodologies presented in this paper can be used for outdoor air quality study purposes, which is a relevant starting point for improving both outdoor and indoor air quality and, therefore, a key-point to achieve smart sustainable cities. These results give insights to researchers and engineers on how to assess wind velocity distribution and mean annual concentrations for comparison with annual regulatory values given by the EU, the WHO or any other organization, and further works could be done to compare the results of the methodologies with monitored data.

Acknowledgments

We would like to thank the ANRT (Association Nationale de la Recherche et de la Technologie) for their support and Météo-France for allowing us to use their data for this study.

DOI : 10.1016/j.scs.2020.102221

References

Anderson, J.O., Thundiyil, J.G., Stolbach, A., 2012. Clearing the Air: A Review of the Effects of Particulate Matter Air Pollution on Human Health. J. Med. Toxicol. 8, 166–175. https://doi.org/10.1007/s13181-011-0203-1

Bai, L., He, Z., Li, C., Chen, Z., 2020. Investigation of yearly indoor/outdoor PM2.5 levels in the perspectives of health impacts and air pollution control: Case study in Changchun, in the northeast of China. Sustainable Cities and Society 53, 101871. https://doi.org/10.1016/j.scs.2019.101871

Bibri, S.E., Krogstie, J., 2017. Smart sustainable cities of the future: An extensive interdisciplinary literature review. Sustainable Cities and Society 31, 183–212. https://doi.org/10.1016/j.scs.2017.02.016

Blocken, B., 2015. Computational Fluid Dynamics for urban physics: Importance, scales, possibilities, limitations and ten tips and tricks towards accurate and reliable simulations. Building and Environment 91, 219–245. https://doi.org/10.1016/j.buildenv.2015.02.015

Buccolieri, R., Santiago, J.-L., Rivas, E., Sanchez, B., 2018. Review on urban tree modelling in CFD simulations: Aerodynamic, deposition and thermal effects. Urban Forestry & Urban Greening 31, 212–220. https://doi.org/10.1016/j.ufug.2018.03.003

Chaloulakou, A., Mavroidis, I., Gavriil, I., 2008. Compliance with the annual NO2 air quality standard in Athens. Required NOx levels and expected health implications. Atmospheric Environment 42, 454–465. https://doi.org/10.1016/j.atmosenv.2007.09.067

EU, 2008. Directive 2008/50/EC of the european parliament and of the council of 21 May 2008 on ambient air quality and cleaner air for Europe, European Union.

Franke, J., Hellsten, A., Schlünzen, H., Carissimo, B., 2007. Best practice guideline for the CFD simulation of flows in the urban environment. COST Action 732.

Jenkin, M.E., 2004. Analysis of sources and partitioning of oxidant in the UK—Part 1: the NOX-dependence of annual mean concentrations of nitrogen dioxide and ozone. Atmospheric Environment 38, 5117–5129. https://doi.org/10.1016/j.atmosenv.2004.05.056

Jurado, X., Reiminger, N., Vazquez, J., Wemmert, C., Dufresne, M., Blond, N., Wertel, J., 2020. Assessment of mean annual NO2 concentration based on a partial dataset. Atmospheric Environment 221, 117087. https://doi.org/10.1016/j.atmosenv.2019.117087

DOI : 10.1016/j.scs.2020.102221

Kim, K.-H., Kabir, E., Kabir, S., 2015. A review on the human health impact of airborne particulate matter. Environment International 74, 136–143. https://doi.org/10.1016/j.envint.2014.10.005

Kumar, M.B.H., Balasubramaniyan, S., Padmanaban, S., Holm-Nielsen, J.B., 2019. Wind Energy Potential Assessment by Weibull Parameter Estimation Using Multiverse Optimization Method: A Case Study of Tirumala Region in India. Energies 12, 2158. https://doi.org/10.3390/en12112158

Mahmood, F.H., Resen, A.K., Khamees, A.B., 2019. Wind characteristic analysis based on Weibull distribution of Al-Salman site, Iraq. Energy Reports S2352484719308716. https://doi.org/10.1016/j.egyr.2019.10.021

Qu, Y., Milliez, M., Musson-Genon, L., Carissimo, B., 2012. Numerical study of the thermal effects of buildings on low-speed airflow taking into account 3D atmospheric radiation in urban canopy. Journal of Wind Engineering and Industrial Aerodynamics 104–106, 474–483. https://doi.org/10.1016/j.jweia.2012.03.008

Reiminger, N., Vazquez, J., Blond, N., Dufresne, M., Wertel, J., 2020. CFD evaluation of mean pollutant concentration variations in step-down street canyons. Journal of Wind Engineering and Industrial Aerodynamics 196, 104032. https://doi.org/10.1016/j.jweia.2019.104032

Richards, P.J., Norris, S.E., 2011. Appropriate boundary conditions for computational wind engineering models revisited. Journal of Wind Engineering and Industrial Aerodynamics 99, 257–266. https://doi.org/10.1016/j.jweia.2010.12.008

Rivas, E., Santiago, J.L., Lechón, Y., Martín, F., Ariño, A., Pons, J.J., Santamaría, J.M., 2019. CFD modelling of air quality in Pamplona City (Spain): Assessment, stations spatial representativeness and health impacts valuation. Science of the Total Environment 19.

Santiago, J.-L., Buccolieri, R., Rivas, E., Sanchez, B., Martilli, A., Gatto, E., Martín, F., 2019. On the Impact of Trees on Ventilation in a Real Street in Pamplona, Spain. Atmosphere 10, 697. https://doi.org/10.3390/atmos10110697

Schatzmann, M., Leitl, B., 2011. Issues with validation of urban flow and dispersion CFD models. Journal of Wind Engineering and Industrial Aerodynamics 99, 169–186. https://doi.org/10.1016/j.jweia.2011.01.005

Ścibor, M., Balcerzak, B., Galbarczyk, A., Targosz, N., Jasienska, G., 2019. Are we safe inside? Indoor air quality in relation to outdoor concentration of PM10 and PM2.5 and to characteristics of homes. Sustainable Cities and Society 48, 101537. https://doi.org/10.1016/j.scs.2019.101537

Shaw, C., Boulic, M., Longley, I., Mitchell, T., Pierse, N., Howden-Chapman, P., 2020. The association between indoor and outdoor NO2 levels: A case study in 50 residences in

DOI : 10.1016/j.scs.2020.102221

an urban neighbourhood in New Zealand. Sustainable Cities and Society 56, 102093. https://doi.org/10.1016/j.scs.2020.102093

Solazzo, E., Vardoulakis, S., Cai, X., 2011. A novel methodology for interpreting air quality measurements from urban streets using CFD modelling. Atmospheric Environment 45, 5230–5239. https://doi.org/10.1016/j.atmosenv.2011.05.022

Toparlar, Y., Blocken, B., Maiheu, B., van Heijst, G.J.F., 2017. A review on the CFD analysis of urban microclimate. Renewable and Sustainable Energy Reviews 80, 1613–1640. https://doi.org/10.1016/j.rser.2017.05.248

Vachon, G., Louka, P., Rosant, J.-M., Mestayer, P.G., Sini, J.-F., 2002. Measurements of Traffic-Induced Turbulence within a Street Canyon during the Nantes'99 Experiment, in: Sokhi, R.S., Bartzis, J.G. (Eds.), Urban Air Quality — Recent Advances. Springer Netherlands, Dordrecht, pp. 127–140. https://doi.org/10.1007/978-94-010-0312-4_10

Vranckx, S., Vos, P., Maiheu, B., Janssen, S., 2015. Impact of trees on pollutant dispersion in street canyons: A numerical study of the annual average effects in Antwerp, Belgium. Science of The Total Environment 532, 474–483. https://doi.org/10.1016/j.scitotenv.2015.06.032

Wang, P., Zhao, D., Wang, W., Mu, H., Cai, G., Liao, C., 2011. Thermal Effect on Pollutant Dispersion in an Urban Street Canyon. International Journal of Environmental Research 5, 813–820. https://doi.org/10.22059/ijer.2011.388

WHO, 2017. Evolution of WHO air quality guidelines past, present and future, Copenhagen: WHO Regional Office for Europe.

Yang, J., Shi, B., Shi, Y., Marvin, S., Zheng, Y., Xia, G., 2020. Air pollution dispersal in high density urban areas: Research on the triadic relation of wind, air pollution, and urban form. Sustainable Cities and Society 54, 101941. https://doi.org/10.1016/j.scs.2019.101941

Yuan, J., Chen, Z., Zhong, L., Wang, B., 2019. Indoor air quality management based on fuzzy risk assessment and its case study. Sustainable Cities and Society 50, 101654. https://doi.org/10.1016/j.scs.2019.101654